

Controlled full adder or subtractor by vibrational quantum computingL. Bomble,¹ D. Lauvergnat,¹ F. Remacle,² and M. Desouter-Lecomte^{1,2,*}¹*Laboratoire de Chimie Physique, Bât 349, Université de Paris-Sud, UMR8000, Orsay F-91405, France*²*Département de Chimie, B6c, Université de Liège, Sart-Tilman, B-4000 Liège 1, Belgium*

(Received 18 January 2009; published 24 August 2009)

A controlled full addition or subtraction can be realized by a unitary transformation on a register of four qubits. The fourth qubit is then used as a control qubit to enforce the addition or the subtraction of two binary digits and a carry or a borrow. The transformation can be decomposed into six elementary gates. The network differs from the adder network of four elementary gates by including two new controlled-NOT gates. The scheme is general and its implementation using vibrational computing has the advantage that the single global transformation that connects the inputs to the outputs can be driven in one step by a single laser shot. This decreases the time of operation and allows for a better use of the optical resources and for an improvement of the fidelity. The laser pulses are optimized by optimal control theory.

DOI: [10.1103/PhysRevA.80.022332](https://doi.org/10.1103/PhysRevA.80.022332)

PACS number(s): 03.67.Ac, 03.67.Lx, 34.50.Ez, 82.50.Nd

I. INTRODUCTION

The implementation of logical gates on a single molecule for classical Boolean logic or quantum computing is receiving growing interest. Classical gates have been realized using optical, electro-optical, redox, and chemical addressing [1–13]. Classical logic functions have also been implemented on the electronic quantum states of a single molecule [14,15] or of a single dopant atom in a fin-type field-effect transistor (FinFET) [16] by electrical addressing. The realization of a quantum computer exploiting entangled states is also a well-recognized topic with numerous theoretical studies [17–21] and potential experimental applications. Various devices have already been proposed based on nuclear magnetic resonance [22,23], optical network [24], electrodynamic cavity [25], ion-traps [26], atoms in cavity [27], atoms in atom chip [28], and molecular eigenstates in different electronic [29–36], rotation vibration [37,38], or vibrational states belonging to a single potential-energy surface [35,39–54].

We focus here on elementary quantum arithmetic with optical addressing. Recently a classical full adder or subtractor exploiting the molecular response to a given stimulated Raman adiabatic passage (STIRAP) pulse sequence according to its intuitive or counterintuitive order has been proposed [3] and a possible experimental implementation of the adder has been discussed [55]. Arithmetic operations can also be executed by quantum gates, i.e., by unitary transformations among atomic or molecular states steered by designed laser fields. It is worthy to note that arithmetic operations are less demanding than quantum algorithms because the gates involve population inversions only and the reading out never requires the knowledge of the quantum phases. The arithmetic operations can therefore be studied and experimentally implemented at two levels: classical or quantum. At the more demanding quantum level, the quantum phase constraint must be taken into account in the optimization of the pulse so that a phase control is enforced to each transition

required by the gate. This ensures that the pulse can implement the gate transformation on any superposition of the computational basis states [42,51]. Phase control could open the way toward the parallelization of additions or subtractions. In numerical computations, the constraint on the phase is the most difficult to realize. If the phase constraint is not satisfied then only population inversion is realized. When this is the case, a classical and not a quantum gate is implemented by the laser field. However, as an arithmetic network [56] only involves population inversions and never uses superposed states, in this sense the computation is quasi classical [57] and is weakly affected by dephasing. Implementing operations classically has therefore the potential to be more robust and on a short term, has to be potential to be more easily experimentally demonstrated on a molecular system.

In this work we show how to modify the quantum adder [56] that we have recently designed using vibrational computing [54] in order to get a controlled adder-subtractor. According to the value of a control qubit, the same gate field is used to perform either the full addition of two binary digits, A and B , and of a carry in, C_{in} , or the full subtraction $A-B$ with a borrow in B_{in} . The logical scheme is general. The realization proposed here implements the gates by encoding qubits in the states of the SCCl_2 polyatomic molecule which has been already used to simulate quantum computing with excited vibrational states [36]. As in Ref. [36] the gate fields steer population transfer among vibrational states of the ground electronic state via transitions toward an intermediary state of an electronic excited state. The spectrum thus lies in the visible uv range.

The paper is organized as follows. In Sec. II, we give the truth tables of the classical full adder and subtractor, and we present the unitary transformation for a reversible controlled adder-subtractor. We show how it could be factorized into a network of elementary gates. The computational method (optimal control) and the model are summarized in Sec. III. The results of simulations are given in Sec. IV. Concluding remarks and a discussion about the scalability and potential implementation are given in Sec. V.

*mdesoute@lcp.u-psud.fr

TABLE I. Truth table of the classical full adder or subtractor.

C_{in} or B_{in}	A	B	S	C_{out}	D	B_{out}
0	0	0	0	0	0	0
1	0	0	1	0	1	1
0	0	1	1	0	1	1
1	0	1	0	1	0	1
0	1	0	1	0	1	0
1	1	0	0	1	0	0
0	1	1	0	1	0	0
1	1	1	1	1	1	1

II. CONTROLLED ADDER-SUBTRACTOR

The truth tables of the classical full adder or subtractor are given in Table I. There are three inputs: the carry C_{in} or the borrow B_{in} and the two binary digits A and B . For the subtraction A is the minuend and B is the subtrahend. The two outputs are the sum $S=A \oplus B \oplus C_{in}$ and the carry out $C_{out}=AB \oplus C_{in}(A \oplus B)$ or the difference $D=A \oplus B \oplus B_{in}$ and the borrow out $B_{out}=\bar{A}B \oplus C_{in}(\bar{A} \oplus B)$ where $\bar{A}=1 \oplus A$. The classical logic operation is irreversible since some of the outputs are identical for different inputs.

Therefore, four qubits (the three inputs Q_1, Q_2, Q_3 , and an auxiliary qubit Q_4) are necessary to build a reversible truth table for the full adder [54] and the auxiliary qubit Q_4 is then initialized in the logical state 0. We propose to use this fourth qubit as a control qubit. If it is initialized in logical state 0 the transformation will perform an addition while when it is initialized to 1, a subtraction is carried out. Table II gives the unitary transformation of a one-step-controlled adder-subtractor. In input, the carry or the borrow are encoded in the first qubit $Q_1=C_{in}$ or $Q_1=B_{in}$. The two digits A and B are encoded in Q_2 and Q_3 . The auxiliary qubit is initialized by $Q_4=0$ or $Q_4=1$. According to the value of this control qubit the two output qubits are the sum out, $Q_3=S$ and the carry out, $Q_4=C_{out}$ for the adder or the difference, $Q_3=D$ and the borrow out, $Q_4=B_{out}$ for the subtractor. The two other qubits ensure that all the output lines are different as it should be in a reversible process. They contain $Q_1=C_{in}$ and $Q_2=A$ for the adder and $Q_1=\bar{B}_{in}=1 \oplus B_{in}$ and $Q_2=A$ for the subtractor.

Vibrational computing offers the possibility to realize this transformation in one step by a single laser pulse without breaking the logic operation into elementary gates [36,54]. The two main advantages are (i) the processing time is notably reduced so the effect of decoherence is decreased. (ii) Fidelity increases since the final fidelity is approximately the product of the fidelities of the elementary gates.

However, it is interesting to divide this unitary transformation into elementary gates, CNOT (controlled-NOT) and TOFFOLI (controlled-controlled-NOT) gates in order to understand its link with the adder network previously proposed [56]. The gates necessary to carry out the addition with a sequence of elementary gates are shown in Fig. 1. The qubits are initialized by $Q_1=C_{in}$, $Q_2=A$, $Q_3=B$, and $Q_4=0$. The final state of the four qubits is $Q_1=C_{in}$, $Q_2=A$, $Q_3=S$, and $Q_4=C_{out}$. As already suggested in Ref. [56], the subtraction

TABLE II. Truth table of the controlled full adder-subtractor. The upper and lower lines refer to the adder or the subtractor, respectively. The bold lines are the cases simulated in Sec. IV.

	Q_1 C_{in} B_{in}	Q_2 A A	Q_3 B B	Q_4 0 1	Q_1 C_{in} \bar{B}_{in}	Q_2 A A	Q_3 S D	Q_4 C_{out} B_{out}
1		0	0	0		0	0	0
		0	0	1		0	0	0
2		1	0	0		1	0	1
		1	0	1		1	0	1
3		0	0	1		0	0	1
		0	0	1		0	0	1
4		1	0	1		1	0	1
		1	0	1		1	0	1
5		0	1	0		0	1	1
		0	1	0		0	1	1
6		1	1	0		1	1	0
		1	1	0		1	1	0
7		0	1	1		0	1	0
		0	1	1		0	1	0
8		1	1	1		1	1	1
		1	1	1		1	1	1

$A-B$ with a borrow B_{in} could be realized by adequately encoding the inputs A and B and applying the four elementary gates of the adder in the reversed order. Here we demonstrate that it is possible to encode the two digits in the same qubits for both cases and use the same sequence of pulses without reversing the order. The fact that an addition or a subtraction is performed is dictated by the value of the fourth qubit. We propose to modify the adder network so that it can be in-

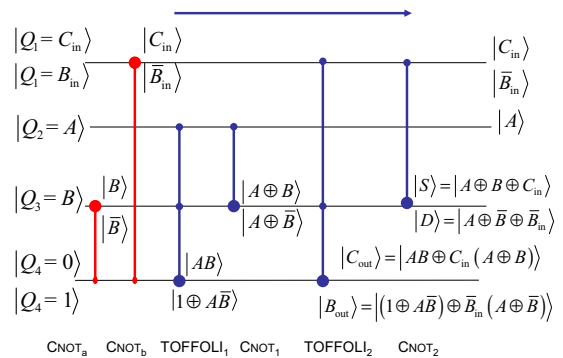


FIG. 1. (Color online) Network for a factorized controlled adder-subtractor. The state of the modified qubit after each gate is written above the line for the adder and below the line for the subtractor. The control qubit Q_4 initially contains 0 for the adder and 1 for the subtractor. The upper arrow indicates the original adder sequence (in blue), the two added CNOT gates are $CNOT_a$ and $CNOT_b$, the first two CNOT on the left (in red).

TABLE III. States of the four qubits after the gates of the controlled adder-subtractor (see Fig. 1). The second column gives the assignment of the qubit states in vibrational states of SCCl_2 (see Sec. IV). The state numbers are those given in Table 1 of Ref. [36]. The bold lines are the cases simulated in Sec. IV.

SCCl ₂ state numbers		CNOT _a	CNOT _b	TOF ₁	CNOT ₁	TOF ₂	CNOT ₂
		$C_{\text{in}} A B 0$					$C_{\text{in}} A S C_{\text{out}}$
1	11	0 0 0 0	0 0 0 0	0 0 0 0	0 0 0 0	0 0 0 0	0 0 0 0
2	1	1 0 0 0	1 0 0 0	1 0 0 0	1 0 0 0	1 0 0 0	1 0 1 0
3	12	0 0 1 0	0 0 1 0	0 0 1 0	0 0 1 0	0 0 1 0	0 0 1 0
4	4	1 0 1 0	1 0 1 0	1 0 1 0	1 0 1 0	1 0 1 0	1 0 0 1
5	2	0 1 0 0	0 1 0 0	0 1 0 0	0 1 0 0	0 1 1 0	0 1 1 0
6	3	1 1 0 0	1 1 0 0	1 1 0 0	1 1 0 0	1 1 1 0	1 1 0 1
7	5	0 1 1 0	0 1 1 0	0 1 1 0	0 1 1 1	0 1 0 1	0 1 0 1
8	8	1 1 1 0	1 1 1 0	1 1 1 0	1 1 1 1	1 1 0 1	1 1 1 1
		$B_{\text{in}} A B 1$					$\bar{B}_{\text{in}} A D B_{\text{out}}$
9	9	0 0 0 1	0 0 1 1	1 0 1 1	1 0 1 1	1 0 1 1	1 0 0 0
10	13	1 0 0 1	1 0 1 1	0 0 1 1	0 0 1 1	0 0 1 1	0 0 1 1
11	15	0 0 1 1	0 0 0 1	1 0 0 1	1 0 0 1	1 0 0 1	1 0 1 1
12	19	1 0 1 1	1 0 0 1	0 0 0 1	0 0 0 1	0 0 0 1	0 0 0 1
13	14	0 1 0 1	0 1 1 1	1 1 1 1	1 1 1 0	1 1 0 0	1 1 1 0
14	18	1 1 0 1	1 1 1 1	0 1 1 1	0 1 1 0	0 1 0 0	0 1 0 0
15	20	0 1 1 1	0 1 0 1	1 1 0 1	1 1 0 1	1 1 1 1	1 1 1 0
16	23	1 1 1 1	1 1 0 1	0 1 0 1	0 1 0 1	0 1 1 1	0 1 1 1

structed to perform either an addition or a subtraction depending on the value of the fourth qubit. This is made possible by adding two new CNOT gates (noted in Fig. 1 CNOT_a and CNOT_b) which have no effect when the fourth qubit Q_4 is in state 0 so that the network performs an addition. On the other hand, when the fourth qubit is in state 1, the network takes the relevant complements so that a subtraction is carried out. When $Q_4=1$, after the two additional CNOT_a and CNOT_b gates, the original adder sequence (see Fig. 1) acts on the four qubits containing: $Q_1=\bar{B}_{\text{in}}$, $Q_2=A$, $Q_3=\bar{B}$, $Q_4=1$. Figure 1 details the action of this extended network according to the value of the control qubit. The results written above or below the line refer to $Q_4=0$ (addition) or $Q_4=1$ (subtraction), respectively. The qubit states after each elementary gate of Fig. 1 are gathered in Table III. The one-step transformation of Table II links the input column and the last one.

III. MODEL AND COMPUTATIONAL DETAILS

According to the optimal control theory (OCT) [58–61] and its generalization for the multitarget case [42], the field optimizes the constrained functional

$$J = \sum_{n=1}^Z \left\{ |\langle \psi_i^n(t_f) | \phi_f^n \rangle|^2 - 2 \operatorname{Re} \left[\int_0^{t_f} \langle \psi_f^n(t) | \partial_t + \frac{i}{\hbar} \hat{H} | \psi_i^n(t) \rangle dt \right] \right\} - \alpha \int_0^{t_f} E^2(t) dt, \quad (1)$$

where α is a positive penalty factor chosen to weight the

importance of the laser fluence. The $\psi_i^n(t)$ are propagated forward in time with initial conditions $\psi_i^n(t=0) = \phi_i^n$, $n = 1, \dots, Z$. The Lagrange multipliers $\psi_f^n(t)$ are propagated backward in time with final conditions $\psi_f^n(t=t_f) = \phi_f^n$, $n = 1, \dots, Z$. Without phase constraint $Z=2^N$ for a N -qubit gate. The ϕ_i^n and ϕ_f^n are then the 2^N initial and final states of the gate transformation. When the phase constraint is taken into account $Z=2^N+1$. The supplementary transition is

$$|\phi_i^{Z=2^N+1}\rangle = \frac{1}{\sqrt{2^N}} \sum_{k=1}^{2^N} |\phi_i^k\rangle \rightarrow |\phi_f^{Z=2^N+1}\rangle = \frac{1}{\sqrt{2^N}} \left(\sum_{j=1}^{2^N} |\phi_f^j\rangle \right) e^{i\varphi}, \quad (2)$$

where the ϕ_i^n and ϕ_f^n correspond to the 2^N gate transitions and the single phase φ can take any value between 0 and 2π [42]. The gate field is a sum of Z contributions

$$E_j(t) = -[s(t)/\hbar\alpha] \operatorname{Im} \left[\sum_{n=1}^Z \langle \psi_f^n(t) | \mu_j | \psi_i^n(t) \rangle \right], \quad (3)$$

where j denotes the polarization direction of the electric field. A switching function $s(t) = \sin^2(\pi t/t_f)$ is introduced to provide a smooth on and off of the field [41]. At each iteration, the field is given by $E_j^{(k)} = E_j^{(k-1)} + \Delta E_j^{(k)}$, where $\Delta E_j^{(k)}$ is calculated by Eq. (3). The fidelity of the gate F is given by the average performance index of each transformation

$$F = \frac{1}{Z} \sum_n^Z |\langle \psi_i^n(t_f) | \phi_f^n \rangle|^2. \quad (4)$$

After optimization, we apply a spectral filtering after Fourier transforming the field. The filter is composed of a bandpass including the spectral domain of the model with a smooth cutoff fixed by a sine-squared function. The pulse is optimized again after filtering and the process is iterated until high fidelity is reached and the spectrum becomes satisfactory. This scheme gives a good convergence even if it does not preserve the monotonic convergence. Monotonic behavior could be achieved by a new filtering algorithm recently suggested [62].

As a proof of principle of the controlled adder-subtractor, we choose a model proposed by Weidinger and Gruebele [36] to simulate quantum computing. The computational basis set is an ensemble of vibrational states of the ground electronic state of the molecule SCCl_2 . The idea is to use a gateway state well separated from other vibrational levels ($\pm 100 \text{ cm}^{-1}$) in the excited \tilde{B} state. This state is populated by a high-resolution laser (35125 cm^{-1}) and then shaped pulses (for example π pulses) can initialize the vibrational states of the ground electronic state for computing. The field forces the vibrational population inversion through transitions via the excited state so the spectrum is in the visible uv range. We use the states and transition moments given in Table 1 of Ref. [36] and computed from Ref. [63]. The assignments of the 2^4 qubit states are given in Table III. The qubit states have been assigned by choosing small transition dipole moments for the states $|0000\rangle$ and $|0010\rangle$ which do not change during the process (see Table III). All the 29 states given in Ref. [36] are included in the simulation. The computational basis set is small but allows a first check of feasibility with realistic molecular data. In addition, this model presents the following advantages. It is built from eigenstates of the tetra-atomic molecule computed in full dimensionality. This avoids decoherence effects due to linkage with inactive vibrational modes when the computational basis set involves some normal modes only. The radiative lifetimes, τ , from the excited gateway state to the vibrational states of the ground electronic state are longer than 10^{-7} s so much longer than the duration of the pulse. The radiative lifetimes have been estimated by the inverse of the Einstein A_{ij} coefficient,

$$A_{ij} = \left(\frac{E_j - E_i}{\hbar c} \right)^3 \frac{|\langle \psi_i | \mu | \psi_j \rangle|^2}{3\pi\epsilon_0\hbar},$$

where E_i and E_j are the energies of the molecular system.

IV. SIMULATION OF COMPUTATION

We first show the results for a one-step implementation of the addition-subtraction in Fig. 2. The transformation connects the two columns of Table II and all the transitions are steered by a single laser pulse sometimes called the universal gate pulse. Table IV gives the objective yields $|\langle \psi_i^n(t_f) | \phi_f^n \rangle|^2$ obtained by the single pulse for each pair of input and output.

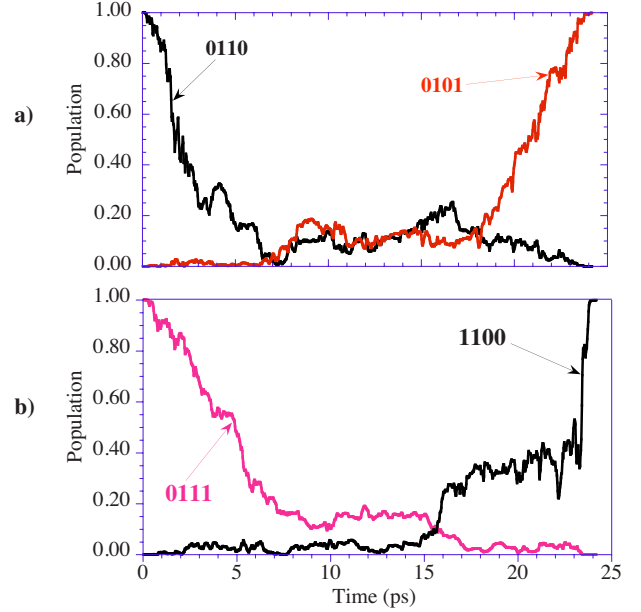


FIG. 2. (Color online) Direct controlled adder-subtractor implemented in the SCCl_2 molecule by OCT with phase constraint. The control qubit is the fourth one. (a) An example of addition ($C_{\text{in}}=0, A=1, B=1, 0 \rightarrow (C_{\text{in}}=0, A=1, \text{the sum is } 0, C_{\text{out}}=1)$) (upper bold line in Table II). (b) Corresponding subtraction ($B_{\text{in}}=0, A=1, B=1, 1 \rightarrow (\bar{B}_{\text{in}}=1, A=1, \text{the difference is } 0, B_{\text{out}}=1)$) (lower bold line in Table II).

Figure 2(a) displays the example ($C_{\text{in}}=0, A=1, B=1, Q_4=0 \rightarrow (C_{\text{in}}=0, A=1, S=0, C_{\text{out}}=1)$) (see upper bold line in Table II) and Fig. 2(b) shows the corresponding subtraction ($B_{\text{in}}=0, A=1, B=1, Q_4=0 \rightarrow (\bar{B}_{\text{in}}=1, A=1, D=0, B_{\text{out}}=1)$) (see lower bold line in Table II). The gate field simultaneously optimizes the 2^N+1 ($N=4$) transformations of Table II with a phase constraint [Eq. (2)]. The transformation is implemented in 24 ps, which is about three times faster than the approach shown in Fig. 5 below where the transformation is implemented by a sequence of pulses, each pulse corresponding to an elementary gate. The average fidelity is 99.6% (see Table IV) and is also significantly better than for an implementation by a sequence of pulses.

TABLE IV. Objective yields for each pair of input and output of the global adder-subtractor implemented in the SCCl_2 molecule by OCT with phase constraint. In bold: the example given in Fig. 2.

Input for addition		Input for subtraction	
0000	99.1	0001	99.8
1000	99.8	1001	99.8
0010	99.2	0011	99.8
1010	99.8	1011	99.8
0100	99.7	0101	99.8
1100	99.9	1101	99.8
0110	99.6	0111	99.9
1110	99.9	1111	99.8
Superposition for phase constraint			97.4

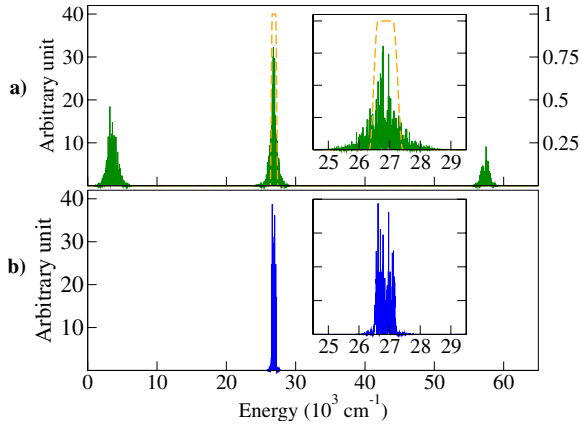


FIG. 3. (Color online) (a) Primary ordinate axis: spectrum (in arbitrary units) of the unfiltered optimal field driving the direct controlled adder-subtractor implemented in the SCl_2 by OCT with phase constraint. Inset with secondary axis: the filtering function in yellow dashed line. (b) Spectrum of the optimal field after filtering.

The trial field for the optimal control contains fourteen frequencies corresponding to transitions involved in the process. The optimization required about 700 iterations. The spectrum of the first optimal field is shown in Fig. 3(a). It contains three bands. The left and right ones are obviously irrelevant. The central band still contains frequencies which do not belong to the spectral range of the model so we apply the filter shown in Fig. 3(a). The fidelity decreases from 99.8% to 69% but the next optimization converges easily in 60 iterations. The spectrum obtained after five cycles of filtering and optimization is shown in Fig. 3(b). This method does not preserve the monotonic convergence but however a good convergence is achieved. The corresponding field is given in Fig. 4. It leads to a very good fidelity of 99.6%. The final field intensity has a maximum of about $5.6 \times 10^{10} \text{ W cm}^{-2}$ which remains well below the ionization limit estimated to $10^{14} \text{ W cm}^{-2}$. It is worth noting that the filtering enables to reduce the field intensity by two orders of magnitude in this example.

Figure 5 illustrates the controlled addition-subtraction carried out by a sequence of elementary pulses for the same example as in Fig. 2. The six fields have been optimized without phase constraint and without filtering to reduce the

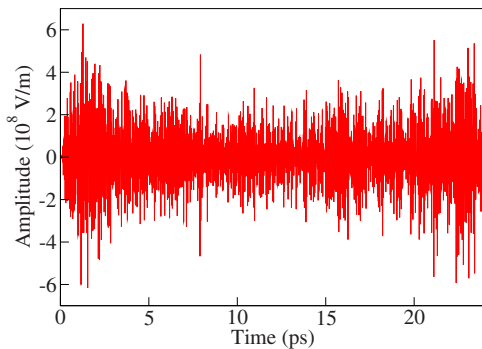


FIG. 4. (Color online) Optimal field of the direct controlled adder-subtractor implemented in the SCl_2 molecule by OCT with phase constraint.

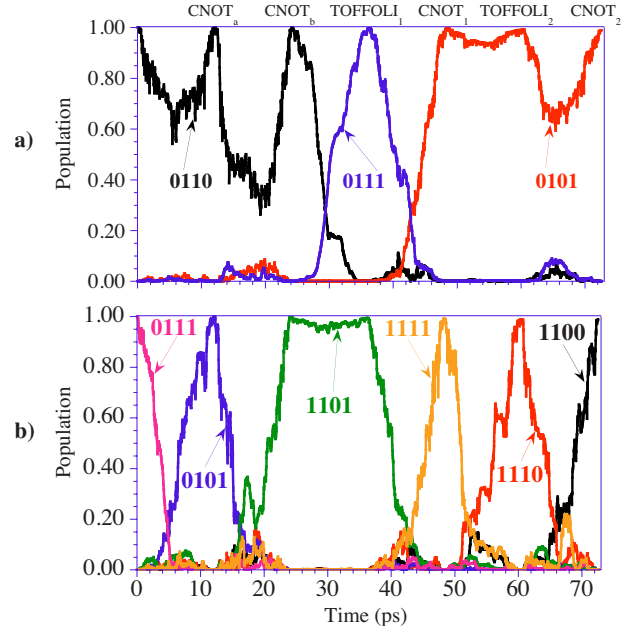


FIG. 5. (Color online) Controlled factorized adder-subtractor implemented in the SCl_2 molecule by OCT without phase constraint. (a) Addition ($C_{in}=0, A=1, B=1, 0 \rightarrow (C_{in}=0, A=1, S=0, C_{out}=1)$ (line 7 of Table III); (b) subtraction ($B_{in}=0, A=1, B=1, 1 \rightarrow (\bar{B}_{in}=0, A=1, D=0, B_{out}=0)$ (line 15 of Table III).

computational time. The previous example has shown that these two improvements could be brought in if necessary. We want to check the feasibility of the concatenation without phase constraint when the fidelity is very high ($>99\%$) for each step of an arithmetic network. The trial field contains eight frequencies for each CNOT gate and four frequencies for the TOFFOLI gates. Figure 5(a) shows the population evolution for the addition ($C_{in}=0, A=1, B=1, Q_4=0 \rightarrow (C_{in}=0, A=1, S=0, C_{out}=1)$ (bold line 7 in Table III) and Fig. 5(b) displays the corresponding subtraction ($B_{in}=0, A=1, B=1, Q_4=0 \rightarrow (\bar{B}_{in}=1, A=1, D=0, B_{out}=1)$ (bold line 15 of Table III). The first gate operates on a given state of the computational basis set. After its operation, if the fidelity is not rigorously 100%, the final state is in principle a superposition of the basis set states; but when the fidelity is very high ($>99\%$), this final state is almost a single basis set state again with an arbitrary phase. One observes that this phase has very little effect on the fidelity of next gate which is again a population inversion. Therefore, when several gates are concatenated the effect of the phase control is expected to be negligible for arithmetic operations if the fidelity is high enough for each step. It is the case for the example of Fig. 5. Obviously this approximation should not be relevant for PHASE or Hadamard gates or for new arithmetic algorithms involving an initial superposition.

The fidelities of each elementary step are gathered in Table V. The average fidelity of the factorized adder-subtractor is now lower (98.8%) and the total time longer (72 ps) than for the one step implementation discussed above. If in addition the simulations are carried out in conditions similar to the one step implementation in order to ensure the phase constraint and a lower field intensity, the elementary pulses will have an even longer duration.

TABLE V. Fidelities of the elementary gates of the controlled adder-subtractor [Eq. (4)].

CNOT _a	99.8
CNOT _b	99.7
TOFFOLI ₁	99.8
CNOT ₁	99.8
TOFFOLI ₂	99.9
CNOT ₂	99.8

V. CONCLUSION

We propose a general logic scheme for an implementation of a controlled full quantum adder or subtractor with a register of four qubits. The value of the control qubit dictates whether an addition $A \oplus B$ or the subtraction $A - B$ of two binary digits with a carry in or a borrow in is to be performed. We show that this unitary transformation can be split in a network of elementary gates. The controlled adder-subtractor is implemented using vibrational qubits which offers the possibility to execute the transformation in one step by a single laser shot. This improves the computational time, reduces the optical resources and increases the fidelity. The feasibility of the process is demonstrated by optimizing the fields by optimal control theory on a realistic molecular system. Exact vibrational states in full dimensionality are used to reduce decoherence due to coupling with inactive modes. The adder-subtractor can be implemented at a classical level which requires populations reading out only. Then the phase constraint in the pulse optimization is not necessary even for the concatenation of the elementary CNOT and TOFFOLI gates when the fidelity is well above 99% for each gate. The phase constraint will however be required for further quantum new algorithms involving superposed states. The phase constraint has therefore been added in some simulations. We note that the pulse filtering allows reducing the intensity of the field needed to realize the addition-subtraction in one step. The optimal fields could further be improved by better filtering [62] or by fitting on sequences of experimentally realizable pulses by adiabatic passage method [37], by genetic algorithm in frequency domain [36,64,65] or ant-colony-optimization algorithm [66].

After illustrating the feasibility of the controlled adder-subtractor on four qubits encoded in a single molecule, the main point will be the concatenation of such processes. Without intermediary reading out, the qubit in which is encoded the carry out or the borrow out must belong to two successive groups of qubits or it must be copied in a qubit of the next group. This obviously raises the problem of scalability and of a relevant physical realization. It is not realistic to increase the number of qubits individually addressable on a single molecule, at least by using the vibrational modes of a single potential energy well, because the number of states, N , needed to build a complex gate increases exponentially as 2^N . The most promising architecture to permit scalable quan-

tum computation is arrays of entities (atoms, ions, or molecules) which can be individually addressed and controlled independently from the states of the other entities but however allow coupling among qubits encoded in neighboring sites. Thus, we have to deal with a subtle intermolecular coupling not too strong to consider individual states as slightly perturbed but sufficiently large to allow an intermolecular gate or to transfer information between entities in a reasonable amount of time. The best situation probably occurs when the intermolecular coupling can be switched on and off [67,68]. In the overall process, this intermolecular step is certainly the bottleneck because it involves a weak-coupling or long-lived rovibrational states. Therefore, it seems crucial to split the overall process in several intramolecular and intermolecular gates. The intramolecular molecular ones will perform as many operations as possible (with a large number of qubits), while the intermolecular gates will be associated with one or two qubits. Trapped ultracold diatomic molecules ($< \mu\text{K}$) present very appealing properties for quantum information processing [69]. They have long-lived rovibrational states and different strategies have already been proposed for intramolecular gates [37,38,64] and for intermolecular gates by using dipole-dipole interactions [67,68,70–72]. Polyatomic molecules have a richer internal structure allowing global gates acting on several qubits as illustrated in this work and one can expect the formation of trapped ultracold molecule ($< \mu\text{K}$) in a near future. Trapped ultracold triatomic ions have already been produced [73]. For neutral molecule, the state of the art is cooling by different experimental techniques ($< \text{mK}$) but not yet trapping [74]. For instance ND_3 has been cold by a Stark decelerator [75]. On the other hand, one may expect that it will be possible to deposit arrays of molecules on surfaces since assembling molecules to get functionalized surfaces is a subject of growing attention. The intermolecular distance should be shorter than for diatomic molecules trapped in an electromagnetic cavity and allow intermolecular transformations by optimal control [70]. The communication between neighboring trapped sites in cavities is expected to be the longer step which could reach the μs . Another possibility could be the cycling of the process on a single entity deposited on a surface if one could find a reading out process operating in a shorter time scale. However, the concatenation without intermediary reading remains more attractive.

ACKNOWLEDGMENTS

The computing facilities of IDRIS (Projects No. 061247 and No. 20060811429) as well as the financial support of the FNRS in the University of Liège SUN Nic2 projects are gratefully acknowledged. We are thankful for the support of the COST Action CM0702 CUSPFEL. The work of F.R. was supported by the EC STREP FP7 project MOLOC and FNRS-FRFC 2.4.565.06. We thank the support of the COST Action CM0702 CUSPFEL and of the Triangle de la Physique, convention No. 20009-039T.

- [1] K. L. Kompa and R. D. Levine, Proc. Natl. Acad. Sci. U.S.A. **98**, 410 (2001).
- [2] F. Remacle and R. D. Levine, J. Chem. Phys. **114**, 10239 (2001).
- [3] F. Remacle and R. D. Levine, Phys. Rev. A **73**, 033820 (2006).
- [4] D. Steinitz, F. Remacle, and R. D. Levine, ChemPhysChem **3**, 43 (2002).
- [5] A. Prasanna de Silva and N. D. McClenaghan, J. Am. Chem. Soc. **122**, 3965 (2000).
- [6] M. N. Stojanovic and D. Stefanovic, J. Am. Chem. Soc. **125**, 6673 (2003).
- [7] J. Andreasson, G. Kodis, Y. Terazono, P. A. Liddell, S. Bandyopadhyay, R. H. Mitchell, T. A. Moore, A. L. Moore, and D. Gust, J. Am. Chem. Soc. **126**, 15926 (2004).
- [8] J. Andreasson, S. D. Straight, G. Kodis, C. D. Park, M. Ham-bourger, M. Gervaldo, B. Albinsson, T. A. Moore, A. L. Moore, and D. Gust, J. Am. Chem. Soc. **128**, 16259 (2006).
- [9] D. Margulies, G. Melman, and A. Shanzer, J. Am. Chem. Soc. **128**, 4865 (2006).
- [10] U. Pischel, Angew. Chem., Int. Ed. **46**, 4026 (2007).
- [11] H. Salman, Y. Eichen, and S. Speiser, Mater. Sci. Eng., C **26**, 881 (2006).
- [12] R. Baron, O. Lioubashevski, E. Katz, T. Niazov, and I. Willner, Angew. Chem., Int. Ed. **45**, 1572 (2006).
- [13] G. Periyasamy, J. P. Collin, J. P. Sauvage, R. D. Levine, and F. Remacle, Chem.-Eur. J. **15**, 1310 (2009).
- [14] S. Ami, M. Hliwa, and C. Joachim, Chem. Phys. Lett. **367**, 662 (2003).
- [15] I. Duchemin and C. Joachim, Chem. Phys. Lett. **406**, 167 (2005).
- [16] M. Klein, G. P. Lansberger, J. A. Mol, S. Rogge, R. D. Levine, and F. Remacle, ChemPhysChem **10**, 162 (2009).
- [17] R. Feynman, Int. J. Theor. Phys. **21**, 467 (1982).
- [18] D. Deutsch, Proc. R. Soc. London, Ser. A **400**, 97 (1985).
- [19] L. K. Grover, Phys. Rev. Lett. **79**, 325 (1997).
- [20] M. A. Nielsen and I. Chuang, *Quantum Computation and Quantum Information* (Cambridge University Press, Cambridge, England, 2000).
- [21] G. Benenti, G. Casati, and G. Strini, *Principles of Quantum Computation and Information* (World Scientific, Singapore, 2004).
- [22] Z. L. Madi, R. Bruschiweiler, and R. R. Ernst, J. Chem. Phys. **109**, 10603 (1998).
- [23] D. Suter and T. S. Mahesh, J. Chem. Phys. **128**, 052206 (2008).
- [24] G. A. Barbosa, Phys. Rev. A **73**, 052321 (2006).
- [25] M. Brune, F. Schmidt-Kaler, A. Maali, J. Dreyer, E. Hagley, J. M. Raimond, and S. Haroche, Phys. Rev. Lett. **76**, 1800 (1996).
- [26] J. I. Cirac and P. Zoller, Phys. Rev. Lett. **74**, 4091 (1995).
- [27] N. Sangouard, X. Lacour, S. Guérin, and H. R. Jauslin, Phys. Rev. A **72**, 062309 (2005); X. Lacour, S. Guérin, N. V. Vitanov, L. P. Yatsenko, and H. R. Jauslin, Opt. Commun. **264**, 362 (2006); X. Lacour, N. Sangouard, S. Guérin, and H. R. Jauslin, Phys. Rev. A **73**, 042321 (2006).
- [28] E. Charron, M. A. Cirone, A. Negretti, J. Schmiedmayer, and T. Calarco, Phys. Rev. A **74**, 012308 (2006).
- [29] J. P. Palao and R. Kosloff, Phys. Rev. Lett. **89**, 188301 (2002).
- [30] J. P. Palao and R. Kosloff, Phys. Rev. A **68**, 062308 (2003).
- [31] J. Vala, Z. Amitay, B. Zhang, S. R. Leone, and R. Kosloff, Phys. Rev. A **66**, 062316 (2002).
- [32] E. A. Shapiro, I. Khavkine, M. Spanner, and M. Y. Ivanov, Phys. Rev. A **67**, 013406 (2003).
- [33] I. R. Sola, V. S. Malinovsky, and J. Santamaria, J. Chem. Phys. **120**, 10955 (2004).
- [34] Y. Ohtsuki, Chem. Phys. Lett. **404**, 126 (2005).
- [35] Y. Teranishi, Y. Ohtsuki, K. Hosaka, H. Chiba, H. Katsuki, and K. Ohmori, J. Chem. Phys. **124**, 114110 (2006).
- [36] D. Weidinger and M. Gruebele, Mol. Phys. **105**, 1999 (2007).
- [37] C. Menzel-Jones and M. Shapiro, Phys. Rev. A **75**, 052308 (2007).
- [38] K. Shioya, K. Mishima, and K. Yamashita, Mol. Phys. **105**, 1283 (2007).
- [39] C. M. Tesch, L. Kurtz, and R. de Vivie-Riedle, Chem. Phys. Lett. **343**, 633 (2001).
- [40] C. M. Tesch and R. de Vivie-Riedle, Phys. Rev. Lett. **89**, 157901 (2002).
- [41] B. M. R. Korff, U. Troppmann, K. L. Kompa, and R. de Vivie-Riedle, J. Chem. Phys. **123**, 244509 (2005).
- [42] C. M. Tesch and R. de Vivie-Riedle, J. Chem. Phys. **121**, 12158 (2004).
- [43] U. Troppmann and R. de Vivie-Riedle, J. Chem. Phys. **122**, 154105 (2005).
- [44] C. Gollub, U. Troppmann, and R. de Vivie-Riedle, New J. Phys. **8**, 48 (2006).
- [45] D. Babikov, J. Chem. Phys. **121**, 7577 (2004).
- [46] S. Suzuki, K. Mishima, and K. Yamashita, Chem. Phys. Lett. **410**, 358 (2005).
- [47] D. Sugny, C. Kontz, M. Ndong, Y. Justum, G. Dive, and M. Desouter-Lecomte, Phys. Rev. A **74**, 043419 (2006).
- [48] D. Sugny, M. Ndong, D. Lauvergnat, Y. Justum, and M. Desouter-Lecomte, J. Photochem. Photobiol., A **190**, 359 (2007).
- [49] M. A. Nielsen, M. R. Dowling, M. Gu, and A. C. Doherty, Phys. Rev. A **73**, 062323 (2006).
- [50] T. Cheng and A. Brown, J. Chem. Phys. **124**, 034111 (2006).
- [51] M. Zhao and D. Babikov, J. Chem. Phys. **125**, 024105 (2006).
- [52] M. Zhao and D. Babikov, J. Chem. Phys. **126**, 204102 (2007).
- [53] M. Ndong, D. Lauvergnat, X. Chapuisat, and M. Desouter-Lecomte, J. Chem. Phys. **126**, 244505 (2007).
- [54] L. Bomble, D. Lauvergnat, F. Remacle, and M. Desouter-Lecomte, J. Chem. Phys. **128**, 064110 (2008).
- [55] L. Bomble, B. Lavorel, F. Remacle, and M. Desouter-Lecomte, J. Chem. Phys. **128**, 194308 (2008).
- [56] V. Vedral, A. Barenco, and A. Ekert, Phys. Rev. A **54**, 147 (1996).
- [57] F. Remacle and R. D. Levine, Proc. Natl. Acad. Sci. U.S.A. **101**, 12091 (2004).
- [58] W. Zhu, J. Bottina, and H. Rabitz, J. Chem. Phys. **108**, 1953 (1998).
- [59] W. Zhu and H. Rabitz, J. Chem. Phys. **109**, 385 (1998).
- [60] Y. Ohtsuki, G. Turicini, and H. Rabitz, J. Chem. Phys. **120**, 5509 (2004).
- [61] Y. Ohtsuki, Y. Teranishi, P. Saalfrank, G. Turicini, and H. Rabitz, Phys. Rev. A **75**, 033407 (2007).
- [62] C. Gollub, M. Kowalewski, and R. de Vivie-Riedle, Phys. Rev. Lett. **101**, 073002 (2008).
- [63] B. Strickler and M. Gruebele, Phys. Chem. Chem. Phys. **6**, 3786 (2004).
- [64] M. Tsubouchi and T. Momose, Phys. Rev. A **77**, 052326

- (2008).
- [65] C. Gollub and R. de Vivie-Riedle, *Phys. Rev. A* **78**, 033424 (2008).
- [66] C. Gollub and R. de Vivie-Riedle, *Phys. Rev. A* **79**, 021401(R) (2009).
- [67] S. F. Yelin, K. Kirby, and R. Côté, *Phys. Rev. A* **74**, 050301(R) (2006).
- [68] E. Kuznetsova, R. Côté, K. Kirby, and S. F. Yelin, *Phys. Rev. A* **78**, 012313 (2008).
- [69] L. D. Carr, D. DeMille, R. V. Krems, and J. Ye, *New J. Phys.* **11**, 055049 (2009).
- [70] K. Mishima and K. Yamashita, *J. Chem. Phys.* **130**, 034108 (2009).
- [71] D. DeMille, *Phys. Rev. Lett.* **88**, 067901 (2002).
- [72] E. Charron, P. Milman, A. Keller, and O. Atabek, *Phys. Rev. A* **75**, 033414 (2007); **77**, 039907 (2008).
- [73] B. Roth, P. Blythe, H. Daerr, L. Patacchini, and S. Schiller, *J. Phys. B* **39**, S1241 (2006).
- [74] R. V. Krems, *Phys. Chem. Chem. Phys.* **10**, 4079 (2008).
- [75] C. E. Heiner, H. L. Bethlem, and G. Meijer, *Phys. Chem. Chem. Phys.* **8**, 2666 (2006).